JME

Journal of Mining & Environment,
Vol. 9, No. 4, 2018, 917-940.
DOI: 10.22044/jme.2018.6752.1495

A comparison between knowledge-driven fuzzy and data-driven artificial neural network approaches for prospecting porphyry Cu mineralization; a case study of Shahr-e-Babak area, Kerman Province, SE Iran

B. Shokouh Saljoughi, A. Hezarkhani* and E. Farahbakhsh

Department of Mining and Metallurgy Engineering, Amirkabir University of Technology (Tehran Polytechnic), Tehran, Iran

Received 5 February 2018; received in revised form 14 June 2018; accepted 19 June 2018
Corresponding author: ardehez@aut.ac.ir (A. Hezarkhani).

Abstract
The study area, located in the southern section of the Central Iranian volcano–sedimentary complex, contains a large number of mineral deposits and occurrences which is currently facing a shortage of resources. Therefore, the prospecting potential areas in the deeper and peripheral spaces has become a high priority in this region. Different direct and indirect methods try to predict promising areas for future explorations, most of which are very time-consuming and costly. The main goal of mineral prospecting is applying a transparent and robust approach for identifying high potential areas to be explored further in the future. This work presents the procedure taken to create two different Cu-mineralization prospectivity maps. The first map is created using a knowledge-driven fuzzy technique and the second one by a data-driven Artificial Neural Network (ANN) approach. In this study aim is to investigate the results of applying the ANN technique and to compare them with the outputs of applying the fuzzy logic method. The geo-datasets employed for creating evidential maps of porphyry Cu mineralization include the solid geology map, alteration map, faults, dykes, airborne total magnetic intensity, airborne gamma-ray spectrometry data (U, Th, K and total count), and known Cu occurrences. Based on this study, the ANN technique is a better predictor of Cu mineralization compared to the fuzzy logic method. The ANN technique, due to capabilities such as classification, pattern matching, optimization, and prediction, is useful in identifying the anomalies associated with the Cu mineralization.

Keywords: *Mineral Potential Mapping, Artificial Neural Network, Fuzzy Logic, Cu Mineralization, Shahr-e-Babak.*

1. Introduction

The first stage in a systematic exploration is to prospect a new mineralization in a region of interest which is known as Mineral Potential Mapping (MPM) [1, 2]. MPM is the process of creating a map that illustrates the favorability of mineralization occurrence in a specified area. Identifying high potential areas within a promising region is one of the fundamental objectives in mineral exploration projects [3-5]. In fact, the main purpose of MPM is to minimize cost and time of prospecting as well as maximizing the prospecting benefits of a mineral exploration program [6]. Different exploratory geo-datasets including the geological, geophysical, and geochemical thematic layers are, respectively, collected, processed, and integrated for MPM. Consequently, MPM can be considered as a multiple criteria decision-making (MCDM) procedure, which creates a predictive model to delineate the prospective zones [7-10].

The main object of MPM is to apply a transparent and robust method in order to determine the favorable zones of a specific mineralization. The most important steps in MPM include selecting proper targeting criteria and applying an advanced, robust, and reproducible approach for

deriving the evidential features [4, 5]. Therefore, the methodological aspects and choosing an appropriate algorithm or methodology in order to obtain the spatial relationships between the evidential features and the known deposit locations are very vital. As a result, an accurate mineral potential map is generally achieved depending on the capacity of the algorithm to learn complex relationships between the input evidential features and the occurrence of mineralization as well as the interpretability and transparency of the algorithm used. Furthermore, an easy implementation of the algorithm and the availability of the software tools in practical applications are also important [11, 12].

The most definitive way to know if an area contains mineral deposits is drilling but it is time-consuming and involves high costs along with a trial-and-error process [13]. Consequently, the geological, geochemical, geophysical, and remote sensing data that is related to the mineralization is fed to a prediction algorithm to help mining companies on decision-making for locating the best drill-hole points. Also advances in computer technology play an increasingly important role in MPM [12, 14].

In the past decades, several MPM approaches have been developed in order to deal with multiple datasets or layers of diverse character from various sources, quantitative integration, and evaluation of these layers [15]. These approaches can be categorized into three classes including the data-driven, knowledge-driven, and hybrid methods. The Data-driven and empirical techniques like logistic regression [11,15-16], weights of evidence (WofE) [17-20], extended weights of evidence [21], evidential belief functions [22-24], fuzzy weights-of-evidence [25, 26], support vector machines [1, 2], fuzzy logic [14], feed-forward neural networks [27], multi-layer perceptrons [28], Bayesian networks [25], radial basis functional link net [29], probabilistic neural networks [30, 31], and restricted Boltzmann machine [32] apply the relationship between the discovered mineral deposits and their surrounding map patterns to create a mineral potential map. The second category, i.e. the knowledge-driven methods, like the fuzzy logic [7, 22, 33-34], Boolean logic [35], wildcat mapping [36], and outranking methods [37] are based on the expert judgment of the analyst. The hybrid methods such as fuzzy WofE modeling [26, 38], data-driven fuzzy modeling [22], and neuro-fuzzy modeling [39] have been proposed in order to optimize the application of both the conceptual knowledge of mineral systems and the empirical spatial associations between mineral deposits and evidential features in geo-computational modelling.

In the recent years, new types of MPM techniques have been developed. These techniques, compared to the conventional ones, assign weights to the continuous spatial evidence without considering the location of known mineral occurrences and expert judgments. Fuzzy logic MPM with continuous evidential data, data-driven index overlay, data-driven Boolean logic, expected value, and geometric average are from these techniques. They are expected to overcome the problem of exploration bias resulting from the expert judgments in knowledge-driven MPM and from using characteristics of known mineral occurrences in data-driven MPM [40, 41].

This study aims to apply the knowledge-driven fuzzy and data-driven ANN models for mineral potential mapping and to compare the outputs with each other. Shahr-e-Babak district in Kerman Province (Iran), which is located in the Cenozoic Sahand-Bazman orogenic belt and has a complex geological setting, was selected as the case study area, and the fuzzy logic and artificial neural networks integration approaches are applied to map Cu mineralization.

This paper is organized as follows: in the next section, the study area is investigated from the aspects of regional geology, structural geology, and geological setting; in Section 3, spatial datasets are described; Section 4 gives an overview of the methods, their principles, advantages, and limitations; Section 5 discusses the results; and finally, in Section 6, conclusions are presented.

2. Study area

Geographically, the study area is situated in the southern section of the Central Iranian Volcanic Sedimentary Complex (Iran). The NE part of the study area is mountainous. It includes Paqaleh range in the east, prominent volcano of Kuh-e-Mosahim in the central part, and Narkuh in the NW. The dasht plain of Shahr-e-babak (Dasht-e Yekkeh Baneh) with an altitude between 1800 and 2000 m is spread in the south and SW part of this area. The drainage pattern is centrifugal in the mountains and mostly parallel in the dasht plain. Rud-e Kang in the west is the most important watercourse. The prevailing part of the sheet territory is drained to the SW [42]. The study area was chosen as a high mineral potential area after a regional Cu potential analysis in the

Shahr-e-Babak district. This region includes many mineral occurrences, and geological, geochemical, and geophysical survey data is available.

The geological map of the study area is depicted in Figure 1, resulted from the geological mapping done by a Yugoslavian group in the 1970s. The oldest units are Cretaceous sediments located in the northernmost part of the sheet (Cenomanian-Turonian flysch often with bioglyphs) and colored mélange formation in the south [42].

The flysch sediments of Eocene age occur in the core of denuded open-anticline axis running NW-SE in the northern part of the study area. The Eocene volcanic-sedimentary unit is the most significant geological unit in the study area which is composed of 80% pyroclastics, 10% lava flows and a remaining 10% sediments [42].

This huge volcano-sedimentary sequence (at least with a thickness of 15 Km) is divided into the Bahr Aseman, Razak, and Hezar complexes by Dimitrijevic et al. (1973) [43].

- The Lower Eocene Bahr Aseman complex begins with several meters thick basal arenites, Pyroclastics, rhyodacite, trachyandesite, andesite, and rhyolite flows.
- Razak complex overlies the Middle Eocene sedimentary sequence. It is divided into 3 units. The lower volcanic unit is mainly basic, the middle one is acidic, and the upper one is mainly basic again.
- Hezar complex represents the youngest phase of Eocene volcanic activity. It is composed of rapidly alternated andesite-basalt, andesite, and rhyolite lava flows.

This Sequence in intrusions dated to Miocene (probably in the time span of uppermost Oligocene to Upper Miocene). Igneous rocks are categorized into two units [43]:

- Granodiorite rocks of Jebal Barez type (granite, granodiorite, quartz diorite, monzonite, and syenite). In the study area, it is represented by the Chenar massif and by several smaller intrusions.
- Kuh-e-Panj type comprises sub-volcanic rocks usually of porphyritic character and strong diversity in composition (quartz diorite, diorite, dacite, etc.). Some volcanic necks in the study area are determined as “dacite and andesite” belonging to this type.

Kuh-e-Mosahim central volcano activity started with a pyroclastic explosion, and continued with deposition of a predominantly pyroclastic material with only several andesite lava flows. Small diorite bodies and dykes crop out in strongly altered rocks in the caldera.

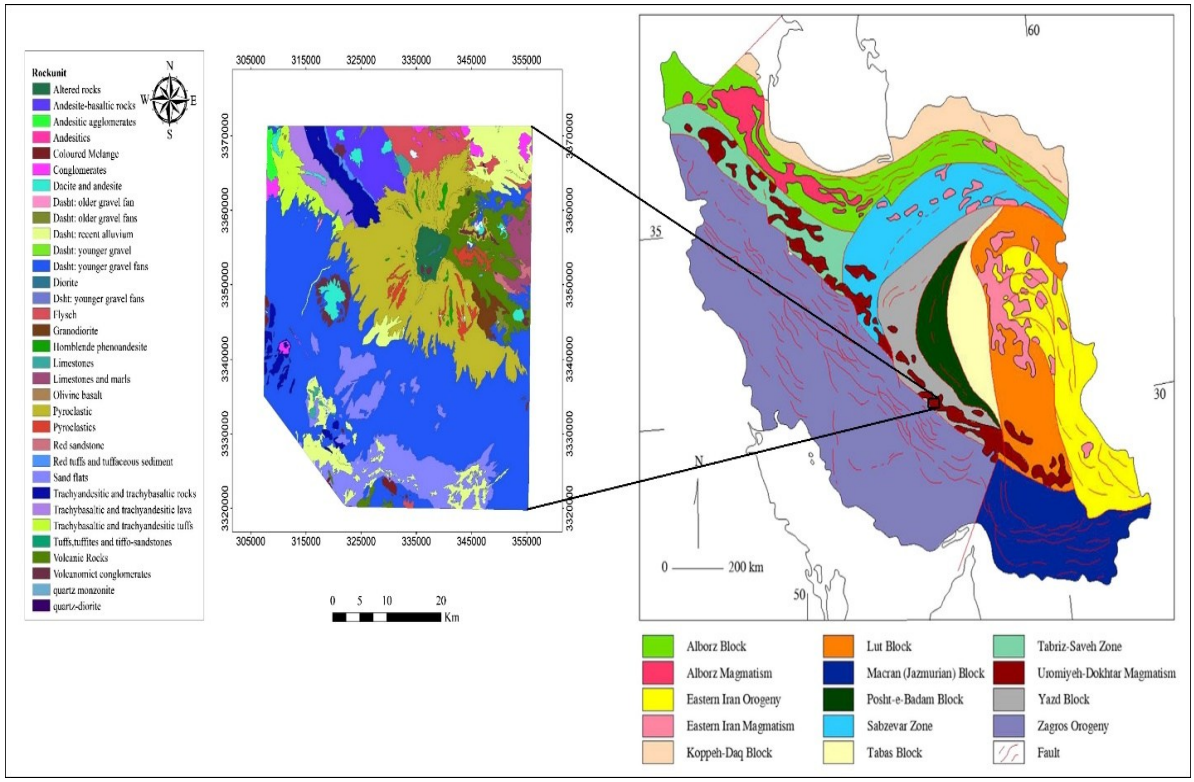

Figure 1. The Urumieh–Dokhtar volcanic belt and associated Cu occurrences in Iran [44], and simplified geological map of the study area [42].

Generally, numerous dykes with an NW-SE strike occurred in the area. The N-S and E-W strikes predominate, respectively, in the northern and eastern parts of the study area. The age of dykes according to some contacts pertains to Eocene up to the youngest volcanic activity of the Pliocene. The composition of the dykes is very variable, but the dacite and andesite dykes are prominent [42].
Structurally, the position of Eocene and Cretaceous flysch in the north-center part of the study area is interpreted as the core of "open" anticline in regional scale. In the SW flank, the important Dehno fault separates Eocene flysch and volcanics. Parallel zone of weakness about 10 km southwestward implicates anomalous readings of scintillometric measurements, confirmed also by the airborne measurements [43]. Miduk district, center (caldera) of the Kuh-e-Mosahim volcano, and also Chenar granitoid massif are situated in this zone [42].
The north part of the study area is subjected to hydrothermal copper and subordinate lead occurrences. The Lachah occurrence is of porphyry copper type, which includes Cu carbonates, chrysocolla, and limonite in the zone of superficial alterations together with primary pyrite and disseminated chalcopyrite. Cu mineralization of vein type occurs at Chah Massi with pyrite, chalcopyrite, and galena as well as in the area of Chehel Dokhtaran (quartz veins containing magnetite and malachite). There is a hydrothermally-altered zone with E-W trending on the southern slopes of Kuh-e-Masahim. A mineralized NNW-SSE fault zone is placed in this part similar to the fault zone located in the south of Kuh-e-sara. The Cu and Pb mineralizations are observed in these zones. The occurrences in the region are concerned with the Neogene volcanism [42].

3. Spatial geo-dataset

The database for the case study corresponds to the Shahr-e-Babak 1:100,000 map sheet, and has been compiled by the Geological Survey of Iran [42]. This area is chosen for a pilot study to test the application of Artificial Neural Network (ANN) for mineral prospectivity mapping. Since this area contains a large number of mineral occurrences, a sufficient number of samples for training are available to apply the ANN method, and later to apply the Fuzzy Logic (FL) method for comparison. Also, all the thematic layers cover the study area uniformly and completely.
The input data to ANN and fuzzy logic (FL) are comprised of solid geology map, alteration map, faults, dykes, airborne total magnetic intensity, airborne gamma-ray spectrometry data (U, Th, K, and total count), and the location of occurrences (Table 1). The occurrence layer includes mineral occurrences and small- and medium-sized mines. Each cell in the gridded data represents a 200 m by 200 m square on the ground.

Table 1. Data layers of the study area.

Category	Factors	Data Type	Scale	Remarks
Occurrence	Cu	Point	-	36 occurrences and mines
Geochemical data	As, B, Ba, Co, Cr, Cu, Mo, Ni, Pb, Sb, Sn, W, Zn	Point	1:100000	IDW (Inverse Distance Weight) interpolation
Geological data	Geology	Polygon	1:100000	Shahr-e-Babak geological map
Faults	Distance from fault	Polyline	1:100000	Fault density map
Dykes	Distance from dyke	Polyline	1:100000	Dyke density map
Geophysical data	Magnetic anomaly	Point	1:100000	IDW interpolation
Airborne gamma ray spectrometry	U, Th, K and total count anomaly	Point	1:100000	IDW interpolation
Satellite data	Alterations	Raster	-	Band ratios

4. Methods

4.1. Artificial Neural Network (ANN) methodology

ANN is a transparent, robust, and reproducible approach, which has been significantly considered by exploration geologists over the past few decades to create mineral potential maps. ANN has a non-linear mathematical structure, which is able to perform any curve-fitting operation in a multi-dimensional space. Hence, it is able to represent an arbitrarily complex data generating process that links the inputs and outputs of that process [45-47].
In the recent years, different types of neural network such as multi-layer perceptrons [28], radial-basis function network [27], probabilistic neural networks [30, 31], and self-organizing map [48] have been applied to mineral potential mapping. Three major components are particularly important in every ANN system

including structure of the nodes, topology of the network, and the learning algorithm used to find the weights of ANN [49, 50]. On the other hand, each processing unit in an ANN, acting as an idealized neuron, receives the input, computes activation, and transmits that activation to other processing units. A weight value, defined to represent the connection strength, is associated with each connection between these processing units. The connection weight of each processing unit is optimally determined through the presentation of known examples and application of a learning rule. Once the connection weight is determined through NN learning, the inter-connection between the input and output embedded in the data is captured [45].

An architecture of ANNs with sigmoid activation function is presented in Figure 2. It contains an input layer, a hidden layer, and an output layer, which are connected by modifiable weights and represented by links between layers. Each input vector is presented with the input layer, and the output of each input unit equals the corresponding elements in the vector. Each hidden unit computes the weighted sum of its input to form its net activation. The subjects mentioned above can be expressed in mathematical terms by Eq. (1):

$$net_j = \sum_{i=1}^{d} x_i w_{ij} + w_{j0} = \sum_{i=0}^{d} x_i w_{ij} \quad (1)$$

where subscripts i and j are, respectively, indices of the units in the input and hidden layers; w_{ij} denotes weights of the input to hidden layer at the hidden unit j, and net_j is the activation for hidden j [45].

Each hidden unit emits an output that is a non-linear function of its activation, f(net), which is shown in Eq. (2):

$$y_j = f(net_j) \quad (2)$$

Each output unit similarly computes its net activation based on the hidden unit signals as Eq. (3):

$$net_k = \sum_{j=1}^{n_H} y_j w_{kj} + w_{k0} = \sum_{j=0}^{n_H} y_j w_{kj} \quad (3)$$

where the subscript k is an index of the units in the output layer and n_H denotes the number of hidden units [45]. An output unit computes the non-linear function of its net, as Eq. (4):

$$z_k = f(net_k) \quad (4)$$

where z_k is the kth output unit. Thus the total network output for a three layers model can be calculated as shown in Eq. (5):

$$z_k = f\left(\sum_{j=1}^{n_H} w_{kj} f\left(\sum_{i=1}^{d} w_{ji} x_i + w_{j0}\right) + w_{k0}\right) \quad (5)$$

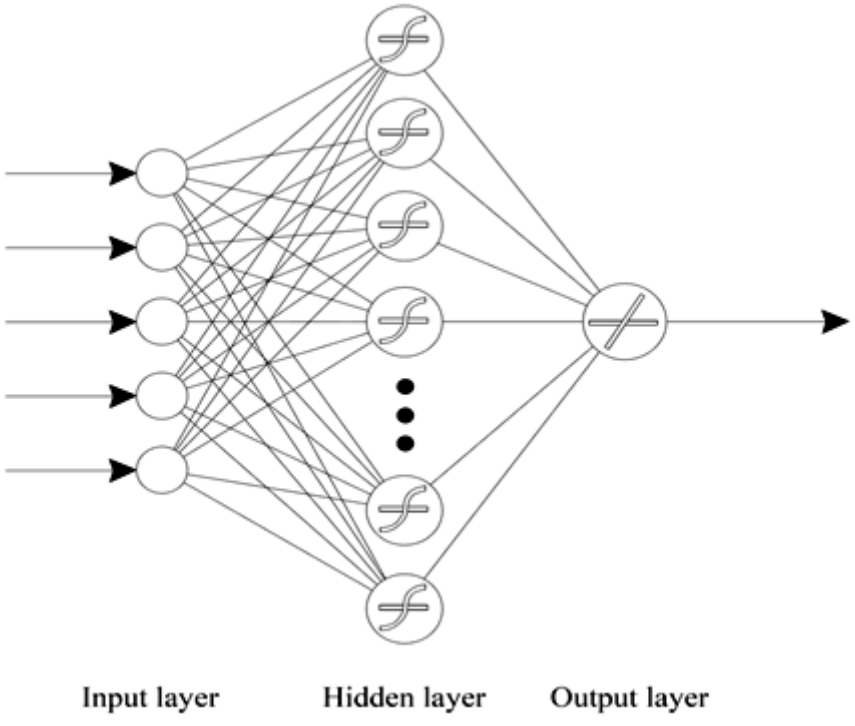

Figure 2. Architecture of ANNs with sigmoid activation function [45].

4.2. Fuzzy Logic (FL) methodology

Similar to ANN, FL is part of a computational intelligence that aims to construct computer systems with human-like ability to reason and make decisions based on the data that is imprecise, subjective or uncertain [51]. FL was first introduced by Zadeh (1965), which is based upon the fuzzy-set theory. Traditionally, this theory is described in association with classical sets. FL does not use a binary response but applies values between 0 (not favorable) and 1 (favorable) [52]. Mathematically, a fuzzy set A in X can be described by Eq. (6) [53]:

$$A = \{x; \mu_A(x)\}, x \in X \quad (6)$$

where $\mu_A(x)$ is the membership value of the element x in the fuzzy set A. The fuzzy membership values are changed from 0 to 1 in a continuous scale, where $\mu_A(x) = 1$ corresponds to full membership of x and $\mu_A(x) = 0$ is equal to non-membership of x in the fuzzy set A. Fuzzy logic represents a conceptual or knowledge-driven approach to mineral prospectivity mapping, which defines the threshold values ranging between 0 and 1, and the fuzzy membership function is applied to each evidential data layer [15]. There are various fuzzy membership functions like linear, Gaussian, small, and large, and each function corresponds to a specific algorithm that is used to fuzzify the input thematic layers. Then the converted evidential data layers as fuzzy subsets are integrated into a unique fuzzy set known as favorability map, which answers the main hypothesis [33].

Data integration is completed following an overlay process, in which the fuzzy subsets are combined by applying fuzzy operators. The most basic operators include AND, OR, Algebraic Sum, Algebraic Product, and fuzzy Gamma operator [54]. The Fuzzy AND represents the minimum operator, and it is equivalent to a Boolean AND operation on a classical set. The Fuzzy OR corresponds to the maximum operator, and it is like the Boolean OR operation. The output of Fuzzy Algebraic Product, which is called a decreasive operator, is always smaller than or equal to the smallest contributing membership value. The fuzzy algebraic sum is complementary to the fuzzy algebraic product, and the output is always larger than or equal to the largest contributing membership value [33].

The fuzzy Gamma represents a combination of the algebraic sum and algebraic product operators, and the degree of combination depends on the Gamma parameter (γ). This parameter is chosen from the range (0, 1): when γ is equal to 1, the output is the same as Algebraic Sum, and when γ is equal to 0, the output is the same as Algebraic Product.

In the recent years, FL has found many applications in the field of exploration geology [55, 56]. In mineral exploration, FL is applied for mineral potential mapping. Different methods have been developed based on FL [7, 22, 33, 34] including fuzzy AHP [57], fuzzy weights of evidence [38, 25], and neuro-fuzzy modelling [39]. We used fuzzy logic and ANN to perform the MPM in the Shahr-e-Babak area, Kerman Province, and eventually, compared the performance of these two methods.

5. Results

5.1. Results of ANN

5.1.1. Data preparation

The most important and time-consuming step in MPM is creating the geo-database. The input layers depending on the data models, structures, and formats can be varied. The evidential maps due to the controlling factors of the porphyry copper mineralization in the Urumieh-Dokhtar magmatic belt include the following thematic layers: solid lithology, tectonic (faults and dykes), airborne total magnetic intensity, airborne gamma-ray spectrometry data (U, Th, K, and total count), remotely-sensed data (hydrothermal alteration haloes), geochemical measurements, and location of the occurrences. After preparing the layers and before further processing, all thematic layers in the geo-database are converted to the raster format. In this study, the 1:100,000 geological map provided by the Geological Survey of Iran (GSI) is used as the lithological layer. The geological base layer involves 23 rock units, many of which have zero or very few deposits. Thus units of the same stratigraphic group are integrated. The result is a simplified geology layer consisting of 9 rock units. The final geologic map is depicted in Figure 3a. The structural data including the map of faults and dykes can be provided by various sources. In this study, they are provided by the geological map and the remotely-sensed data, and then classified and coded based on the strike. The east-trending lineaments are highly related to the porphyry copper occurrences in the Kerman region [43]. Thus linear features including faults and dykes are extracted from the geological map and modified considering the Landsat 8 satellite image. Then the densities of faults and dykes are mapped. The layer of faults and dykes is also converted to a

grid in which the cell values indicate the distance to the nearest fault (Figures 3b, c). Airborne magnetic data is the other dataset used in this study. This dataset has been acquired by the Atomic Energy Organization of Iran (AEOI) during 1977 and 1978. Airborne magnetic data has been acquired from the flight lines at 500 m spacing and altitude of 120 m.

Interpretation of the airborne geophysical data related to the local mines and exploration geology helps to resolve the broad geology and structural features on the Shahr-e-Babak area, Kerman province, SE Iran. First, the magnetic data has been reduced to the pole using the RTP filter. This method removes the dependence of the magnetic data on inclination. This method simplifies the interpretation procedure since the asymmetric responses of sub-vertical prisms or contacts are transformed to simpler symmetric and anti-symmetric forms. The symmetric "highs" are directly centered on the body, while the maximum gradient of the anti-symmetric dipolar anomalies coincides exactly with the body edges. RTP is performed on the digitized aeromagnetic data of the study area via fast Fourier filtering programs in order to remove the dipolar nature of the magnetic field [58]. Then the analytic signal method is applied on the resulted data from the previous step, and the result obtained is shown in Figure 3d. Remotely-sensed data (ASTER) is used as the other dataset. This layer has been processed after applying the required corrections. The band ratio technique has been applied on the ASTER data to define the alteration haloes around the intrusive bodies [59]. One evidential map is derived from the processed images as the alteration haloes (Figure 3e). The airborne geophysical surveys have also been performed for gamma-spectrometry of uranium, thorium, potassium, and total count. The radiometric data pre-processing is done to detect and remove spikes. This is accomplished using a fourth-difference analysis, in which the value of the radiometric field at a given point is replaced by the differences between the values at the four nearest adjacent points along a given flight line. In the cases where the fourth difference is found to be higher than the standard deviation of the data, the radiometric value is checked for the presence of the positioning or measurement errors. After the spike removal, the data is interpolated using a minimum curvature algorithm [60]. The grid cell size is chosen to be 1/4 of the flight line spacing (i.e. 200 m). By such a cell size, the spectral content of the original field is almost entirely preserved, whereas the aliasing effect is avoided. The results obtained are shown in Figs. 3f, g, h, i.

The stream sediment geochemical data is another dataset used in this study. This dataset is extracted from the 1:100,000 sheet of the Shahr-e-Babak published by GSI. In this study, Factor Analysis (FA) is applied to determine the elemental associations related to the Cu mineralization. First, the data for the selected geochemical elements of Zn, Pb, Cr, Ni, Cu, As, Sb, Co, Sn, Ba, B, W, and Mo is transformed by ilr transformation [61], which eliminates the effects of data closure. Then FA with a varimax rotation for ilr-transformed data is applied. The final map of the stream sediment geochemical data is prepared as an evidential map, which is shown in Figure 3j. The mineral deposit layer includes mineral occurrences and small/medium-sized mines, which is shown in Figure 3k.

The six evidential maps are encoded as class scores were digitally superposed. The statistical description of the data that is applied in this study for both the input and output are shown in Table 2. All evidential maps are combined to generate 62086 six-dimensional feature vectors. Since the operation is carried out in a GIS-based environment, an associated database is automatically generated, which stores the components of the feature vectors. Target vectors define output vectors to which input feature vectors are mapped by an ANN. The input feature vectors with known target vectors constitute the training vectors. The validation vectors that are also known as the target vectors are used exclusively for validating the training of ANN. Regarding mineral potential mapping, there is only one single-dimensional binary target vector encoded as 1 or 0, representing the presence or absence of a target mineral deposit, respectively. Determination of the deposited samples is easy because these samples are the feature vectors corresponding to the location of known mineral deposits. However, the selection of non-deposited samples is somewhat difficult. To this end, the knowledge-based and data-driven methods can be used. In the data-driven approach, the non-deposited samples can be selected randomly from pre-modeled areas with low probability of hosting mined deposits. Also in the knowledge-driven method, using the previous knowledge of the process of forming the target mineral deposit type, the feature vectors of the points that have a very low probability are used as the non-deposit training/validation vectors. The feature vectors corresponding to the presence or absence of a

target mineral deposit constitute the training/validation vectors. These vectors are referred to as the deposit or non-deposit training/validation vectors, respectively. In this work, we used the well-explored parts of the area to select the training and validation data. Therefore, the Miduk site was selected, which has a total of 36 well-known occurrences and deposits (Figure 3k). The above-mentioned materials are shown schematically in Figure 4.

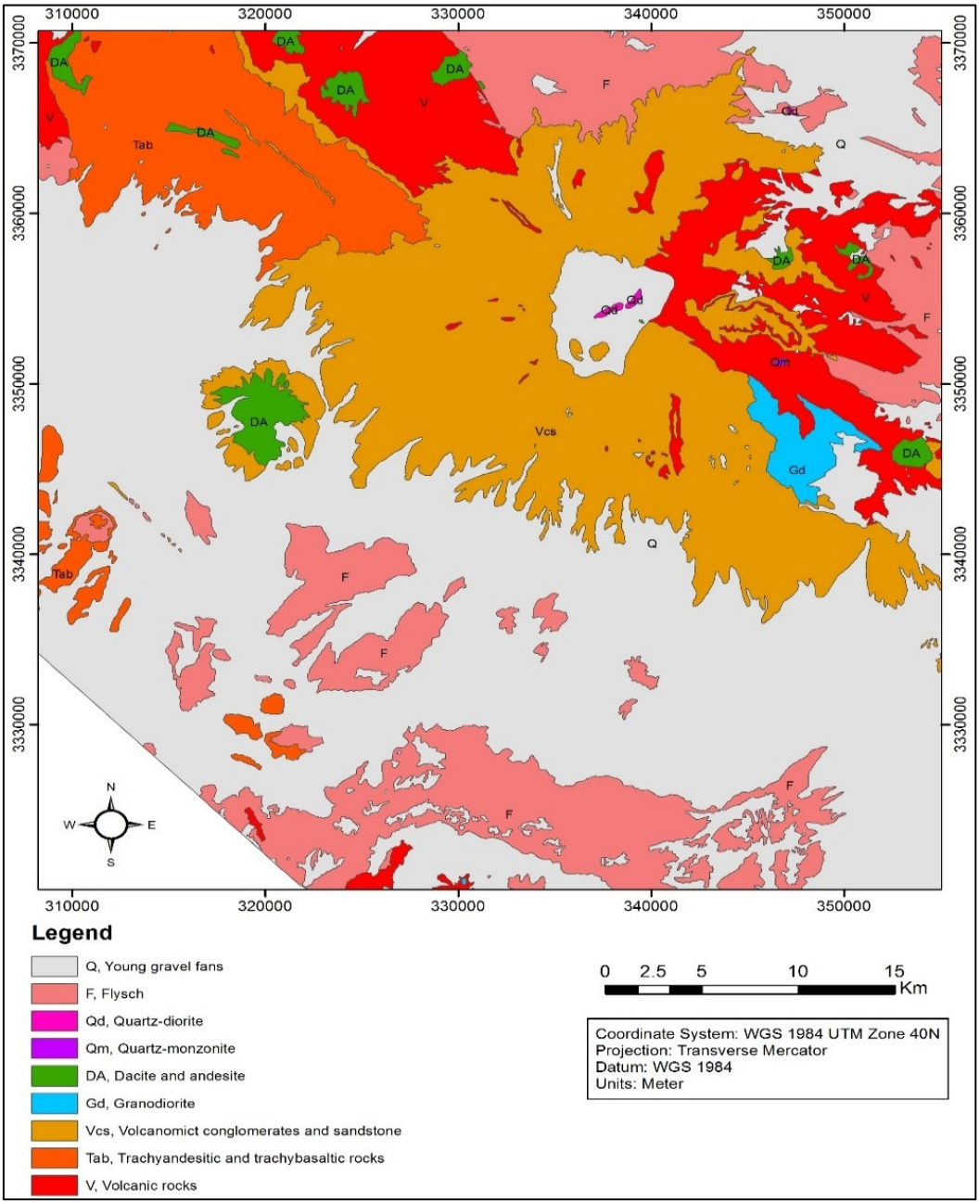

(a)

Figure 3. Evidential layers after processing the primary data. a) lithological map; b) fault density; c) dyke density; d) analytic signal map of the magnetic data; e) hydrothermal alterations extracted from the ASTER satellite data; radiometric data resulting from gamma-spectrometry of potassium (f), uranium (g), thorium (h), total count (i); interpolated map of the factor related to the Cu mineralization resulting from processing the stream sediment samples, k) mineral-deposit locations.

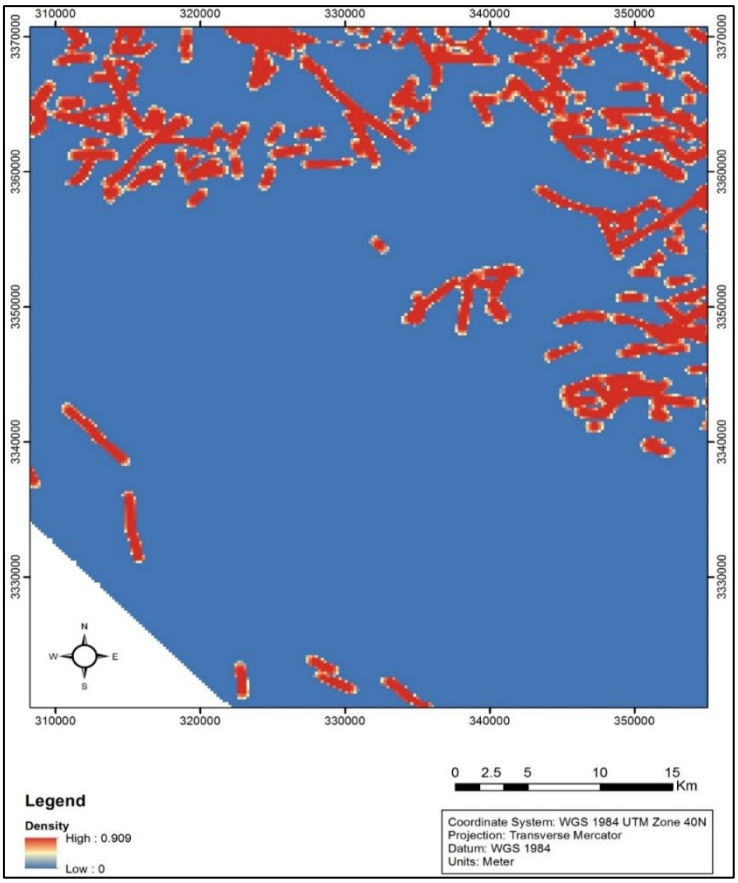

(b)

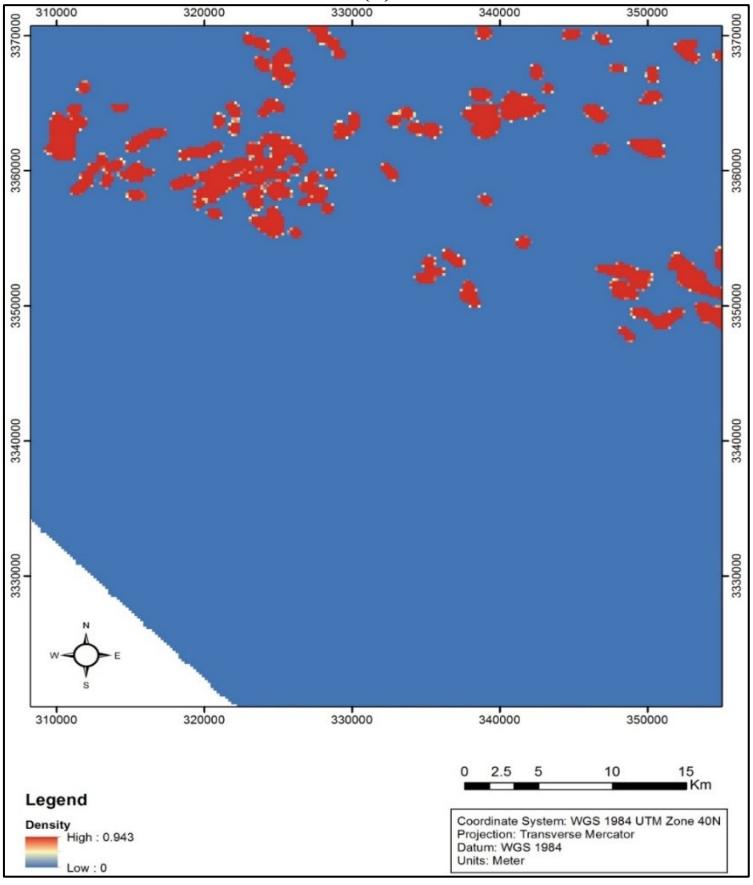

(c)

Figure 3. Continued.

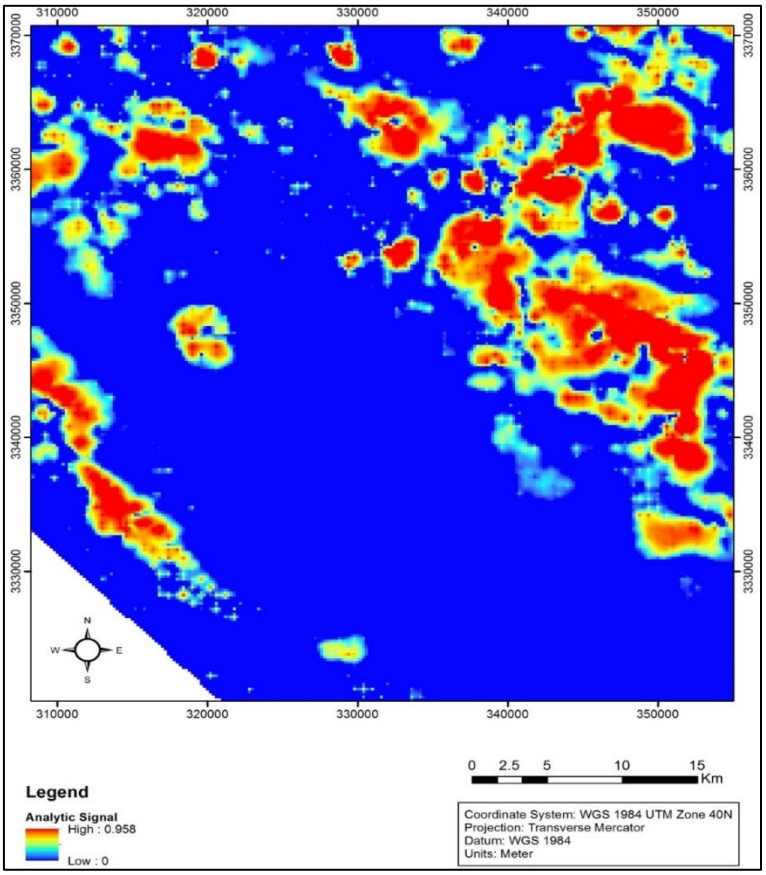

(d)

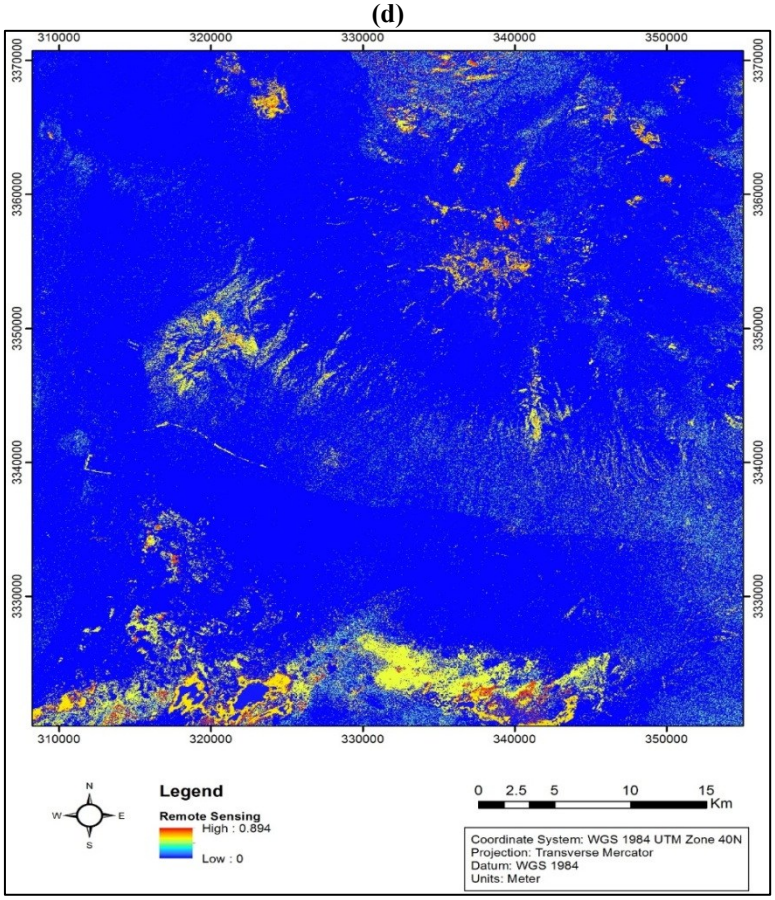

(e)

Figure 3. Continued.

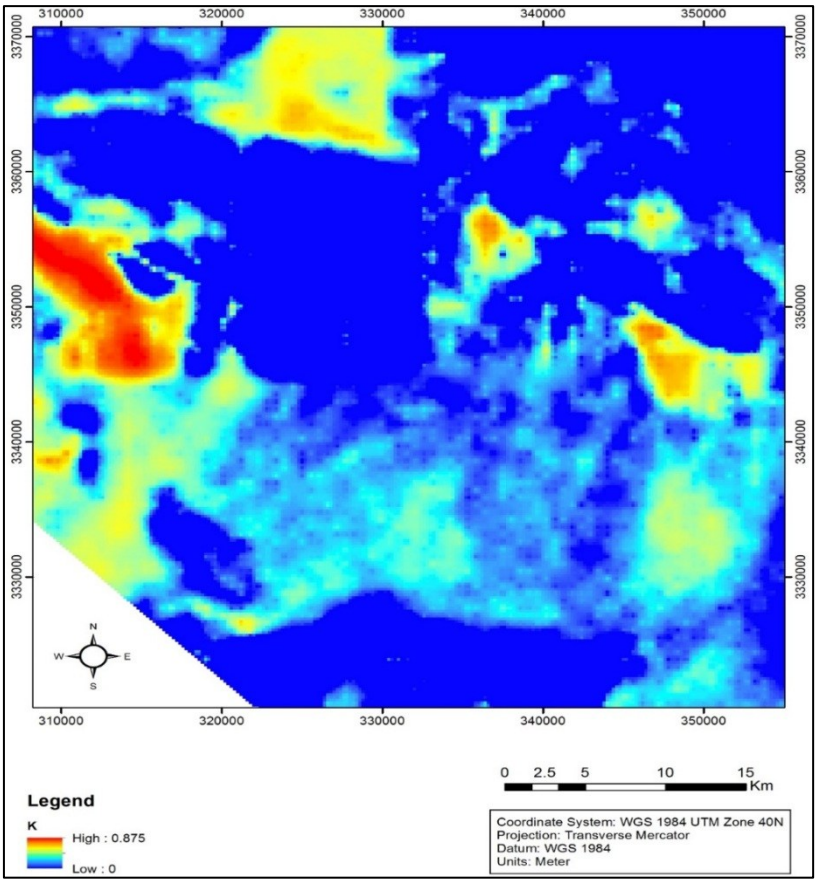

(f)

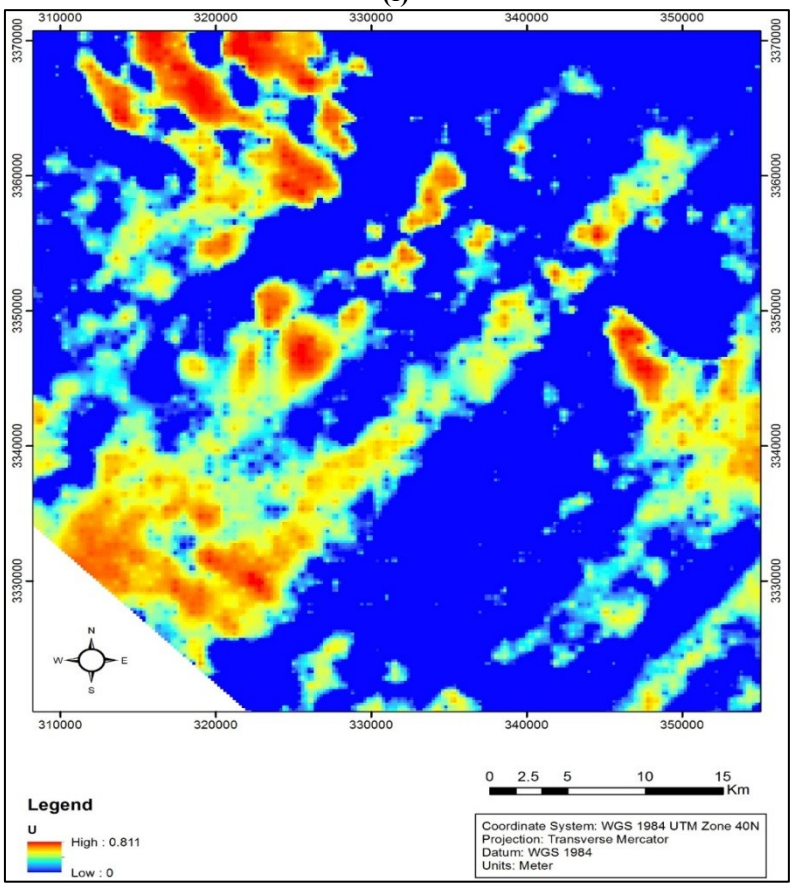

(g)

Figure 3. Continued.

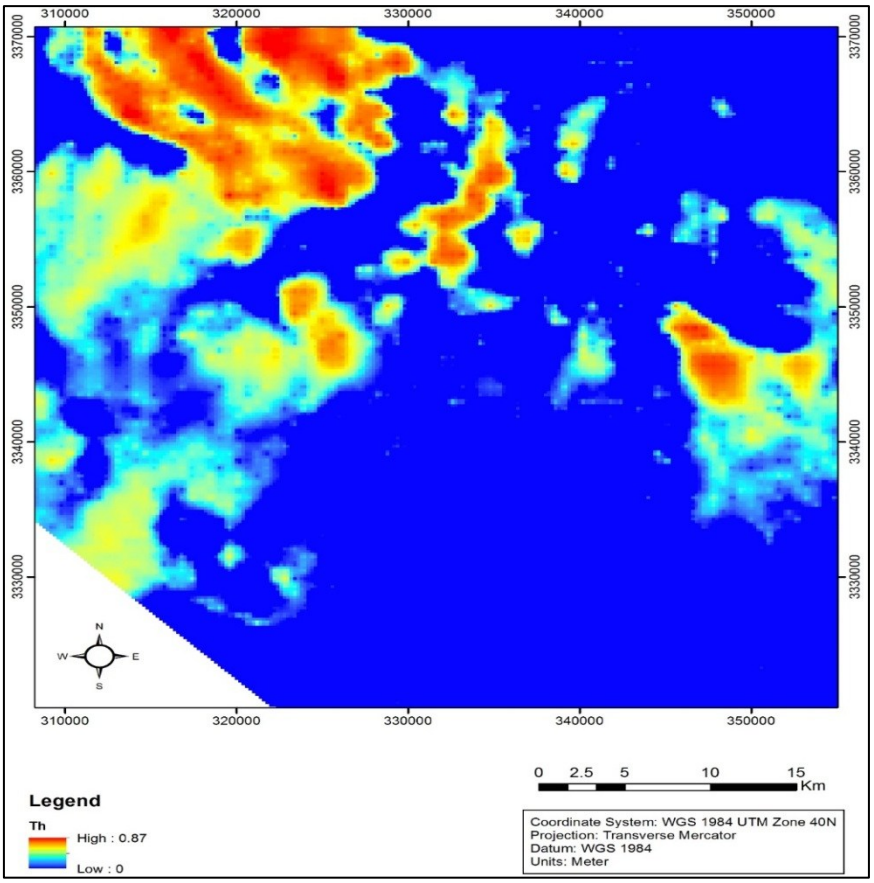

(h)

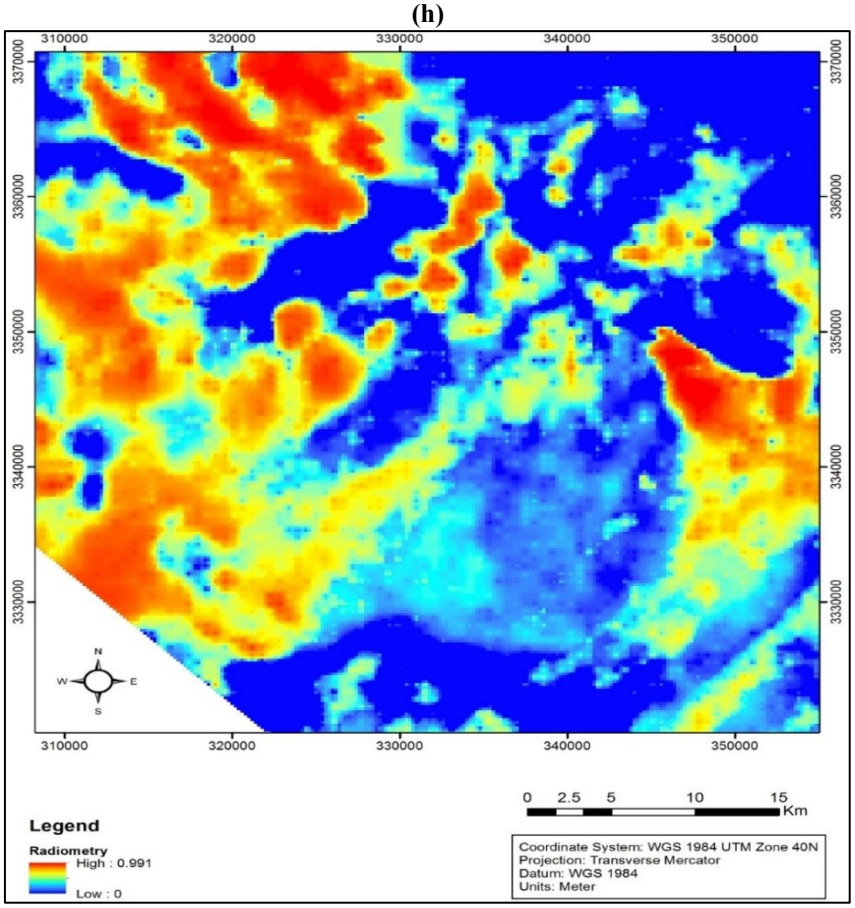

(i)

Figure 3. Continued.

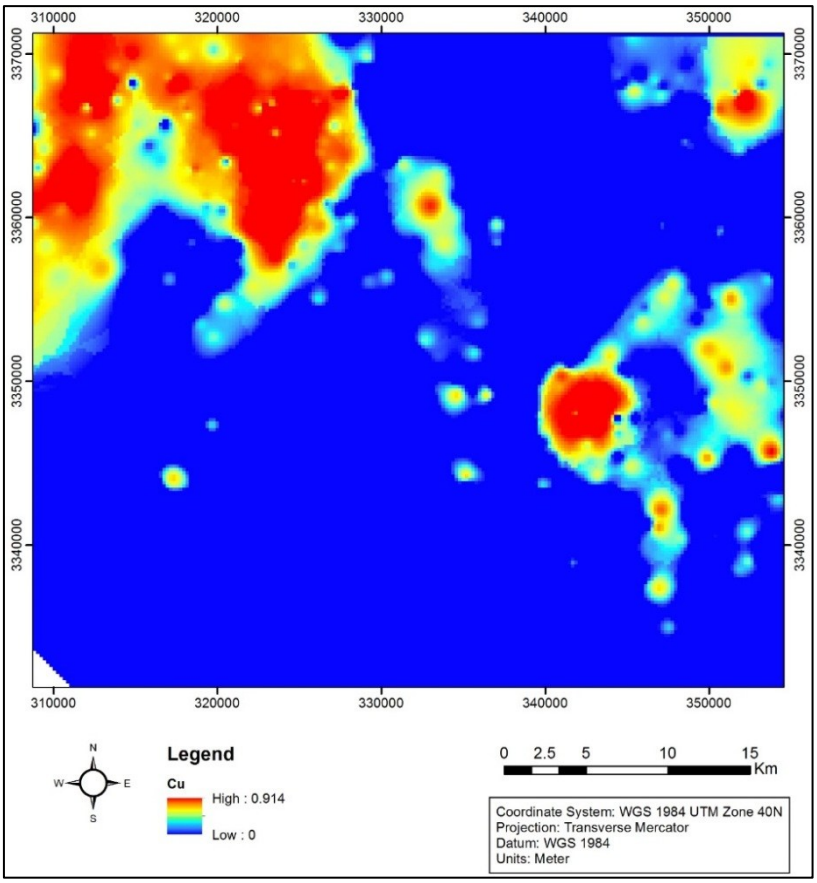

(j)

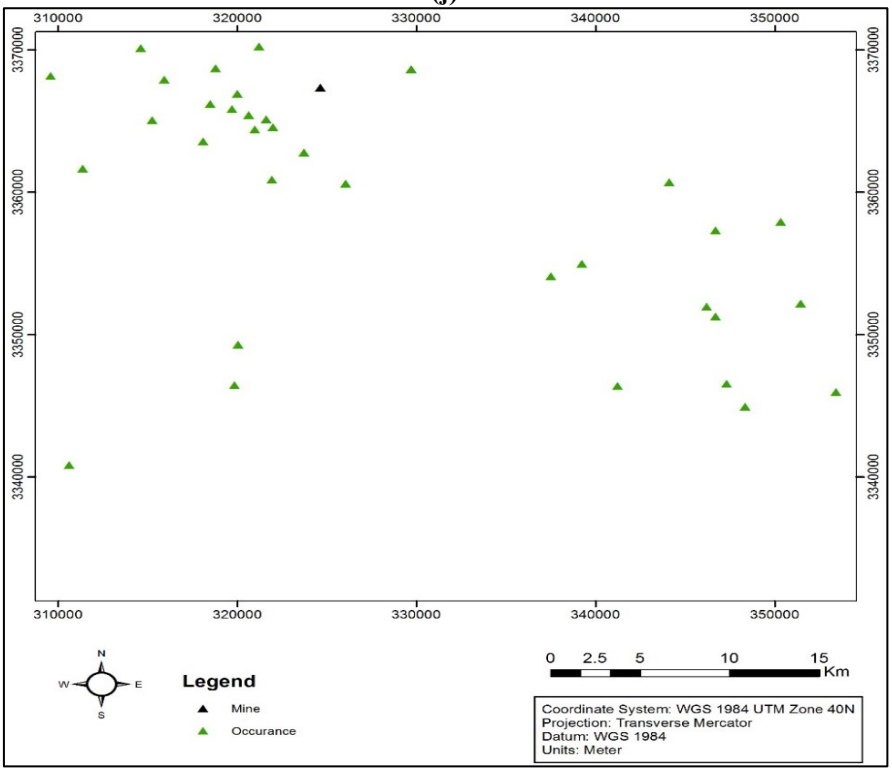

(k)

Figure 3. Continued.

Table 2. Statistical description of the input and output data.

	Layer	Evidential map	Number	Average	Minimum	Maximum	Standard deviation
Inputs	Lithological	Solid geology	62086	-	0.1	0.9	-
	Geochemical	Selected factor score map	62086	-0.098	-0.92	12.55	0.55
	Alteration	Presence and proximity to alteration haloes	62086	-	0	1	-
	Geophysical	Total magnetic intensity	62086	16.06	-10190.81	15149.60	3128.60
		Potassium	62086	64	8.04	185.46	17.36
		Uranium	62086	208.23	23.39	445.25	55.32
		Thorium	62086	592.87	47.02	1884.92	193.08
		Total count	62086	856.38	149.02	2218.68	226.27
	Structural	Fault density	62086	0.191	0	5.55	0.53
		Dyke density	62086	0.059	0	4.32	0.259
Output	Deposit/occurrence location	Mineral deposit location	62086	-	0	1	-

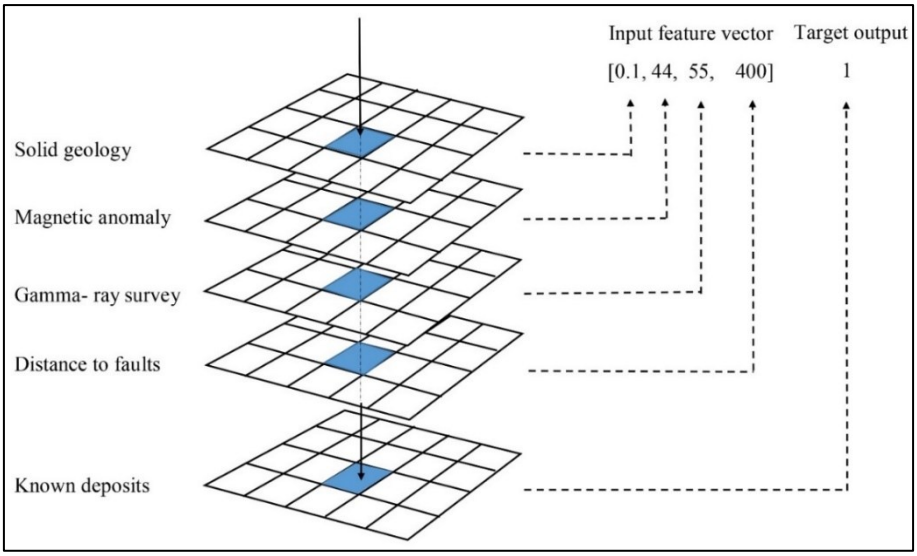

Figure 4. Relationship between GIS thematic layers and feature vectors used as input to the ANN model. For each cell on the Shahr-e-babak grid, the components of the input feature vector for that location are set to the values stored in the thematic layers. Each pattern in the dataset is used to train the network consisting of an input feature vector paired with the desired output (i.e. the value indicating the presence or absence of a deposit).

At the beginning of the ANN modelling, it is necessary that all the evidential layers with continuous values be normalized. It helps to reduce the noises and scale the inputs and output, and consequently, leads to a better prediction. Scaling the inputs and output before applying ANN is very important. The main advantage is to avoid attributes in greater numeric ranges dominating those in smaller numeric ranges. Another advantage is to avoid numerical difficulties during the calculation. Because kernel values usually depend on the inner products of feature vectors, e.g. the linear kernel and the polynomial kernel, large attribute values might cause numerical problems [62, 63]. In the past decades, various normalization methods have been tested to improve the network training [64-66]. In this study, each one of the variables is normalized by applying the following three methods to find the most effective and precise one. These applied methods include the original data, the normalized data that is in the range of [-1, 1] using the maximum and minimum values of the dataset, the normalized data using the mean and standard deviation of the dataset, and finally, the normalized data in the range of [0, 1] using the following equation:

$$X_{norm} = \frac{x - x_{min}}{x_{max} - x_{min}} \quad (7)$$

where x is the input data that should be normalized; x_{max} and x_{min} are the maximum and minimum of the original data, respectively. X_{norm} is also the normalized data that has been transformed. The results obtained indicate that applying Eq. (7) for normalizing leads to better responses. Therefore, in this work, the input and output data is normalized by this method. Only for the lithology layer with the discrete values of 0.1, 0.2, 0.3, 0.4, 0.5, 0.6, 0.7, 0.8, and 0.9, classes are assigned as the 1st to 9th lithology groups, respectively.

5.1.2. Divisionism and performance indices

One of the most important issues in ANN modelling is Divisionism, which helps to make the resulting model logical and accurate. In general, the data can be divided into three categories: 1) training data: this group is characterized definite and clear, and they are used during the training process; 2) test data: their target is not clear, and they are used after the training process; 3) validation data: they are not definite and are used during the training process and to avoid over-fitting. In this study, all the available datasets are divided randomly into three distinct subsets consisting of the training, validation, and testing data. The proportions of each one of these subsets are 70%, 15%, and 15% of the whole number of the data (Table 3).

Table 3. Range of different parameters for training, testing, and validating the datasets.

	Effective parameters		Train data (43460 samples)			Test data (9313 samples)			Validation data (9313 samples)		
			Min*	Ave**	Max***	Min	Ave	Max	Min	Ave	Max
Input parameters	Lithological	Solid geology	0.1	-	0.9	0.1	-	0.9	0.1	-	0.9
	Geochemical	Selected factor score map	-0.86	-0.07	12.55	-0.88	-0.2	1.94	-0.924	-0.093	1.69
	Alteration	Presence and proximity to alteration haloes	0	-	1	0	-	1	0	-	1
	Geophysical	Total magnetic intensity	-7296.73	158.03	11284.76	-10162.89	423.97	10975.31	-10190.81	-1054.27	15149.66
		Potassium	8.04	65.29	18.46	19.74	58.70	97.41	9.36	63.31	118.59
		Uranium	23.39	212.48	444.58	46.41	198.41	328.48	31.16	198.23	445.25
		Thorium	47.02	620.14	1884.92	53.96	525.33	1425.8	148.62	533.19	1198.73
		Total count	149.02	890.63	2218.68	288.43	765.99	1374.68	162.48	786.92	1713.62
	Structural	Fault density	0	0.141	5.55	0	0.384	4.92	0	0.231	3.58
		Dyke density	0	0.05	4.32	0	0.035	2.70	0	0.089	3.32
Output parameter	Deposit/occurrence location	Mineral deposit location	0	-	1	0	-	1	0	-	1

* **Minimum**
** **Maximum**
*** **Average**

According to mineral potential mapping, there is only one single-dimensional binary target vector encoded as one corresponding to the presence and zero equal to the absence of a target mineral deposit. These feature vectors construct the training/validation vectors. The vectors are referred to as the deposit or non-deposit training/validation vectors, respectively. The first subset is the training set by which the network finds an input-output spatial relationship by repetitive analysis of the training set (about 70% of the training/validation dataset). The second and third subsets are the validation and test sets (about 15% of the validation and about 15% of the test dataset).

The performance of the various prediction models like ANN can be assessed in terms of fitting accuracy once each one of the model structures is calibrated using the training/validation dataset and the testing dataset. Also the Root Mean Squared Error (RMSE) between the predicted values from the models and the desired output and the coefficient of determination (R^2) can be used as measures of performance. These two indices are used in this work; R^2 measures the degree of correlation between the observed and predicted values. It measures the strength of the model by

developing a relationship among the input and output variables. R^2 values range from 0 to 1 with 1 indicating a perfect fit between the data and the line drawn through them and 0 representing no statistical correlation between the data and a line. R^2 is given by Eq. (8) [67]:

$$R^2 = 1 - \frac{\sum_{k=1}^{N}(t_k - y_k)^2}{\sum_{k=1}^{N}(t_k - \overline{t}_k)^2} \quad (8)$$

where t_k and y_k are, respectively, the target and network output for the kth input, $\overline{t}_k$ is the average of the targets, and N is the total number of events considered.

The root mean square error (RMSE) evaluates the variance of the errors independently of the sample size, and is given by Eq. (9) [67]:

$$RMSE = \sqrt{\frac{SEE}{N}} \quad (9)$$

where SEE is the sum of the squared errors and N is the number of data points used. SEE is given by Eq. (10):

$$SEE = \sum_{i=1}^{N}(y_i - \overline{y}_i)^2 \quad (10)$$

with the variables having already been defined. RMSE indicates the discrepancy between the observed and forecasted values. A perfect fit between the observed and forecasted values would have an RMSE of 0. The models that minimize the RMSE measures along with the optimum R^2 are selected as the best ones. The whole analysis is repeated for several times.

5.1.3. ANN modelling

ANN models can be viewed as a graphical representation of a parametric function, which takes a set of input values and maps and corresponds them to a set of output values. In this study, a feed forward-scaled conjugate gradient network and feed forward–Levenberg–Marquardt are selected for training. In neural network applied in this study, the sigmoid function is employed as the transfer function for ANN in the hidden layer neurons. MATLAB is utilized for training and testing the networks.

Multi-layer perceptron (MLP) is one of the most prevalent architectures in ANN. This architecture is advantageous from several aspects. Therefore in this work, this network has been evaluated (Figure 5) in order to compare with the output of applying FL. The best feed forward neural network structure is achieved with 7 neurons in its hidden layer (selected based on the trial-and-error), which has sigmoid transfer functions in its hidden layer neurons. Figure 6 illustrates the favorable map resulting from the ANN technique.

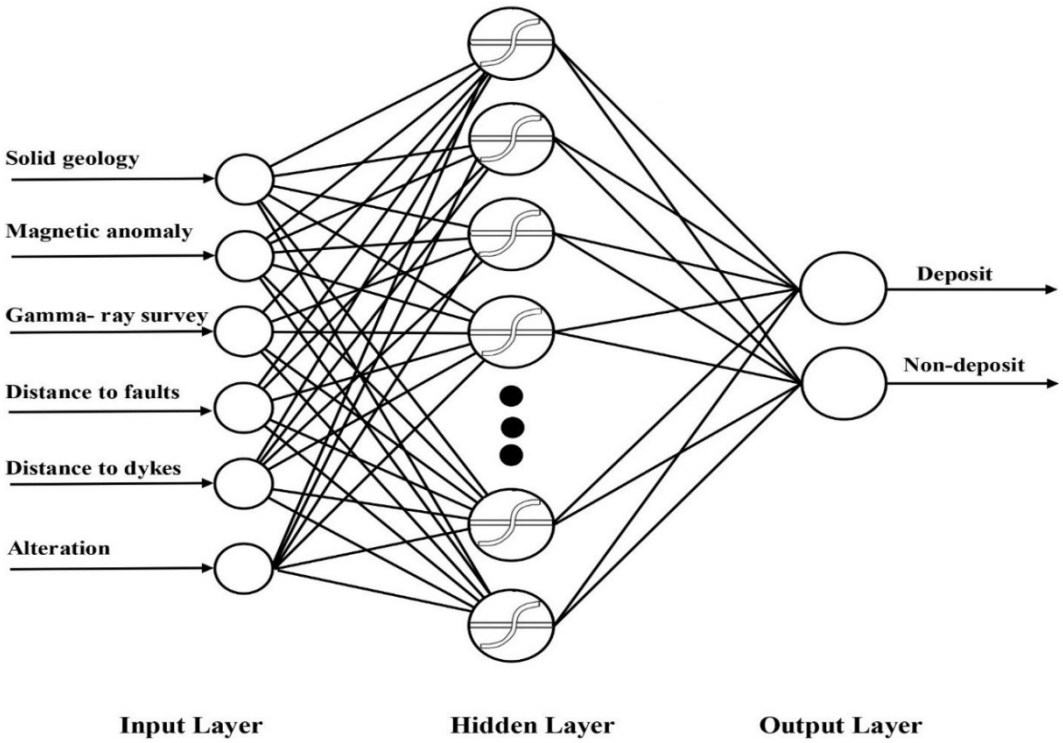

Figure 5. ANN architecture with sigmoid activation function for predicting Cu mineralization.

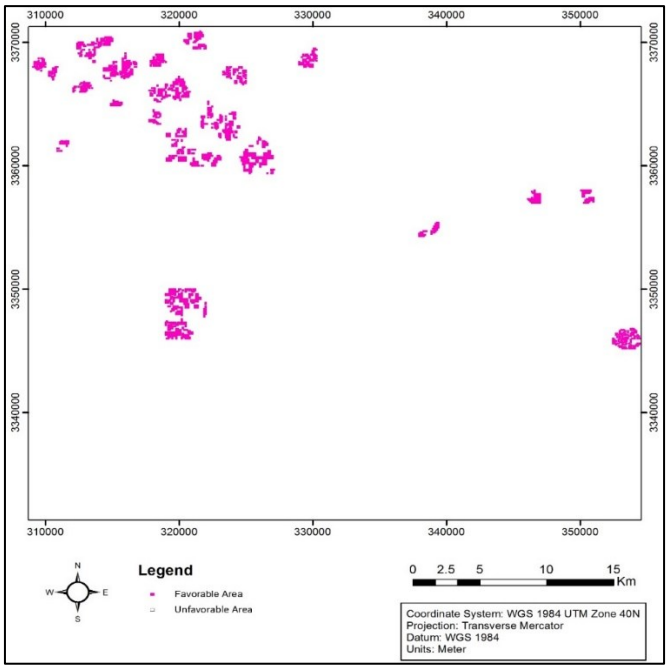

Figure 6. Favorable map resulted from ANN modelling.

5.2. Result of FL method

In this work, the entire FL modelling, as shown in Figure 7, is performed using ArcGIS 10.3 (ESRI software), which is described in the following.

5.2.1. Fuzzification

First, using various fuzzy membership tools, different evidential data layers are converted into fuzzy subsets (Figure 7). The input raster data layer using a particular fuzzification algorithm is transformed into a range from 0 to 1.

5.2.2. Data integration

After applying fuzzy membership algorithms on the evidential data layers, these layers are integrated into the single layer output using fuzzy overlay operators of algebraic product, algebraic sum, and Gamma, as shown in the Figure 8. The fuzzy algebraic sum operator is applied to two weighted structure layers in order to generate a sum map of the structural criterion, and the algebraic product operator is applied to two geological layers for preparing the final map of the geology criterion. As well, the product operator is applied to two geophysical layers for preparing the final map of the geophysical criterion. Subsequently, the fuzzy Gamma operator with different gamma values is used to integrate four layers consisting of one geochemical layer, two fuzzy geophysical layers, geological layer, and two fuzzy structural maps; $\gamma = 0.75$ gives the best result. The resulting mineral potential map for Cu mineralization with the Gamma operator of 0.75 is shown in Figure 9.

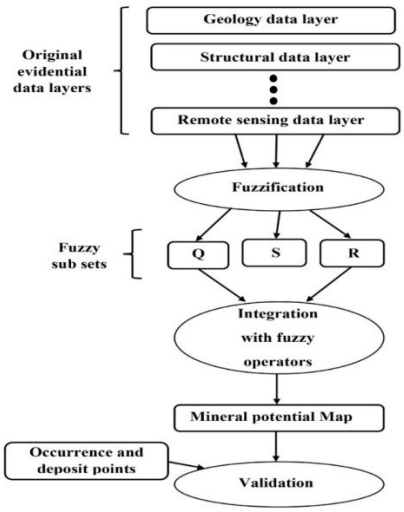

Figure 7. FL modelling steps followed in this study.

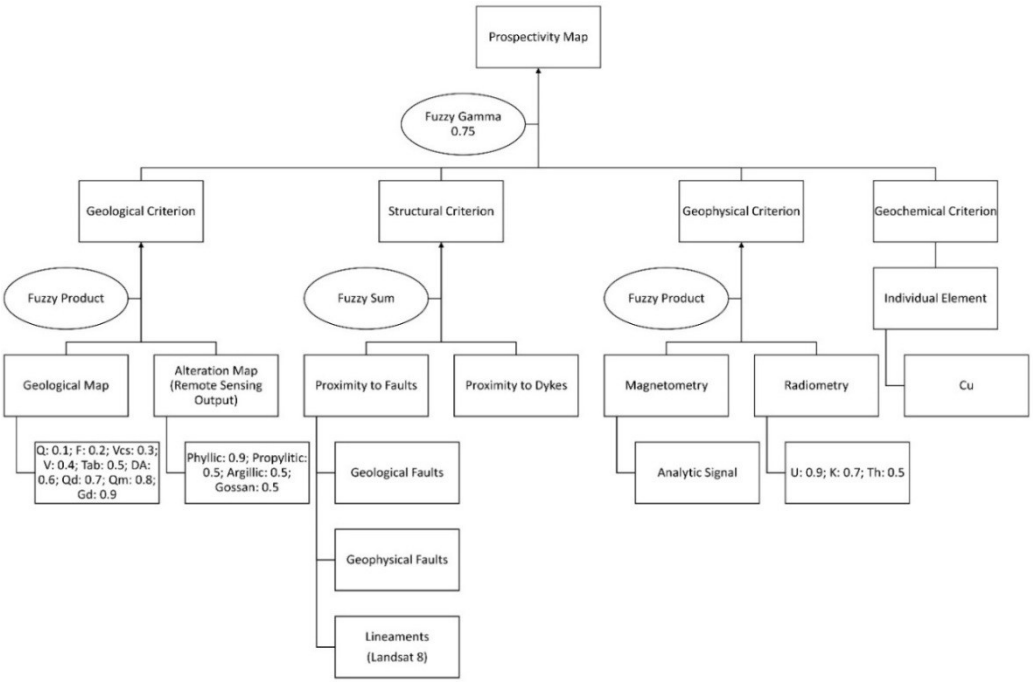

Figure 8. General framework applied for data integration.

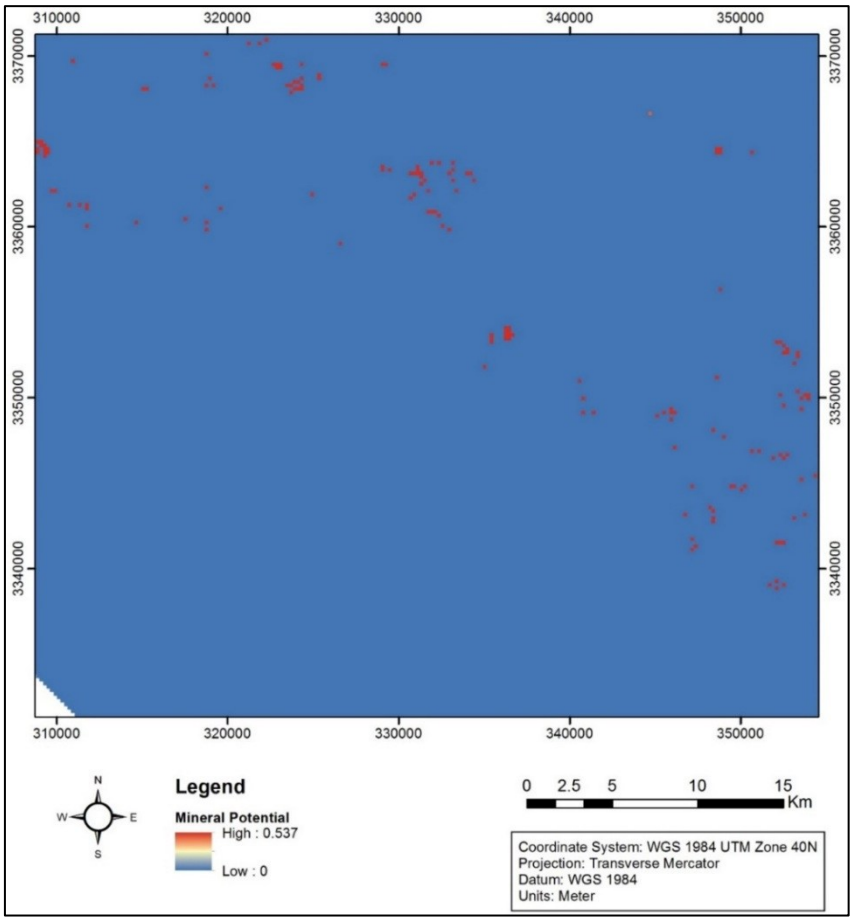

Figure 9. Mineral potential map generated with fuzzy logic: Gamma = 0.75.

6. Discussion

Nowadays, mineral exploration is almost impossible with only one information layer. For this purpose, various data layers such as the geological, geophysical, and geochemical layers have to be considered. Earth science information that is used in mineral potential mapping has an empirical component comprising an exploration

database and a conceptual component comprising an expert knowledge-base [39]. In this work, ANN and FL were used to combine the exploration data in regional-scale for potential mapping of copper mineralization in the Shahr-e-Babak area, Kerman, which has a great potential for porphyry Cu deposits.

ANNs are empirical and data-driven methods that attempt to emulate features of the biological neural networks (i.e. the human brain and nervous system) in order to address a range of difficult information processing, analysis, and modelling problems [68]. They constitute good pattern recognition and classification tools with the ability to generalize from imprecise input data [69]. The advantages of applying ANNs to MPM are: (i) no physics-based algorithm is required to build the model; therefore, the modelling approach is faster and more flexible than the physics-based modelling approaches in most cases; (ii) ANNs can handle non-linear relationships easily and properly; and (iii) the expertise and user experiences may be incorporated easily into the model structure [70]. During the recent years, different types of ANNs have been used more than any other methods in mineral potential mapping [29, 31]; however, there are several problems with ANN's training and designing. Most of the ANNs are time-consuming procedures of architecture design, and these methods learn generally the slow and easy converge to local minima or over-fit. In order to avoid over-fitting, it is necessary to use additional techniques (e.g. cross-validation and regularization), which can give an indication when further training is not resulting in better generalization.

Fuzzy systems like neural networks are a computing paradigm that represent an attempt to build computer systems with a human-like ability to reason and make decisions based on the data that is uncertain, imprecise or subjective [71] Whereas neural networks can learn from data, fuzzy systems require explicit statements of uncertain knowledge as inputs. Therefore, fuzzy systems represent a conceptual or knowledge-driven approach to mineral-prospectivity mapping [72]. In the field of mineral exploitation, several methods based on fuzzy mathematics have been applied to MPM such as FL, fuzzy AHP, and fuzzy weights of evidence [73, 74]. FL refers to the "weights" used in weights of evidence as fuzzy membership values [72]. Fuzzy membership values are dependent on how important the geologist believes a particular geological feature contributes to the mineralization process. The transparency and interpretability of fuzzy systems is often emphasized as one of their key advantages, especially in comparison with the so-called "black-box" approximation methods such as neural networks. Similar to the other approaches, despite its widespread application in MPM, FL has some disadvantages. One of the most important issues in FL is making decision(s) based on appropriate parameters, i.e. MFs, distribution of MFs, and the fuzzy rule compositions [75].

The mineral prospectivity maps produced using the ANN and FL methods are shown, together with known gold occurrence and deposit points, in Figures 10 and 11, respectively. The ANN method produces meaningful results from the geological aspect. The results of applying the ANN method are in good agreement with the known deposits namely Meiduk and Sara. The ANN method is able to predict areas with high, moderate, and low favorability. The results of this method are compared with the FL results. Both methods are in good agreement with areas with high-to-moderate favorability, which are found around the Meiduk and Sara deposits and also at the northern parts of the Abdar deposit. The areas with moderate-to-low favorability are mostly scattered in the west, center, and east to northeast of the study area. These areas are far from the well-known deposits, and are good candidates for further exploration.

In this study, in order to quantitatively validate the results obtained from the two methods, the prediction-area (P-A) plot was used. In the P-A plot, the cumulative percentage of known occurrences predicted by the integration of evidential classes and their corresponding cumulative occupied areas (with respect to the total studied area) are plotted versus the prospectivity values. Thus the prediction ability of the evidential layer and its ability to delimit the studied area for further exploration are evaluated in a scheme [41].

In a P-A plot, there are two curves, the curve of the percentage (prediction rate) of known mineral occurrences corresponding to the classes of the prospectivity map and the curve of the percentage of occupied areas corresponding to the classes of the prospectivity map. When an intersection point of the two curves is at a higher place in the P-A plot, it portrays a small area containing a large number of mineral deposits. Furthermore, it objectively chooses a better model to give priority for mineral exploration [76, 77]. Comparison of

the prediction rates in the P-A plots (Figure 12) shows the importance of analyzing the predictability of prospectivity models. The intersection point in the P-A plot (Figure 11a) of the ANN prospectivity model shows 80% of the known Cu occurrences predicted in 20% of the studied area, while the intersection point in the P-A plot (Figure 11b) of the logic fuzzy prospectivity model shows 70% of the known Cu occurrences predicted in 30% of the studied area. The parameters of the intersection points in the P-A plots of the integrated maps are shown in Table 4. Comparison of the presented data demonstrates a higher efficiency of the prospectivity models generated using ANN integration over the FL prospectivity models.

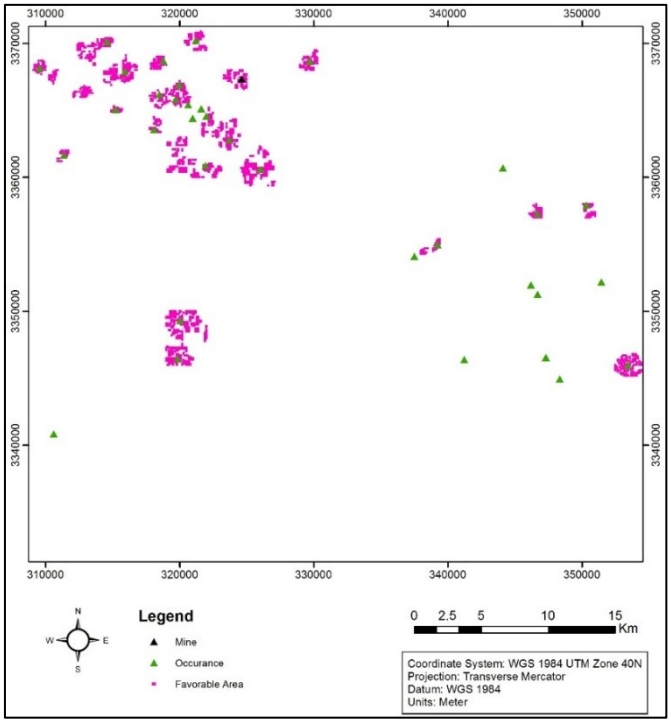

Figure 10. Mineral potential map created by ANN along with the mineral occurrences and mines.

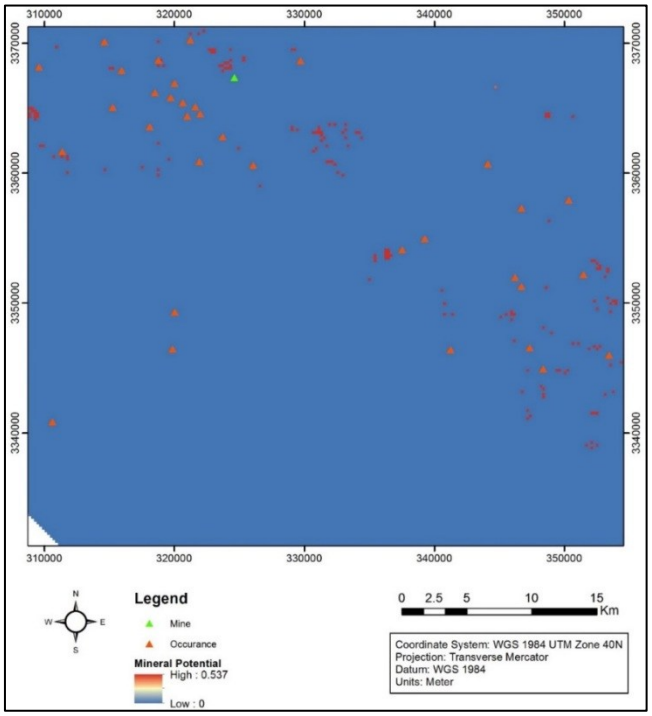

Figure 11. Mineral potential map generated by FL (γ = 0.75) along with the mineral occurrences and mines.

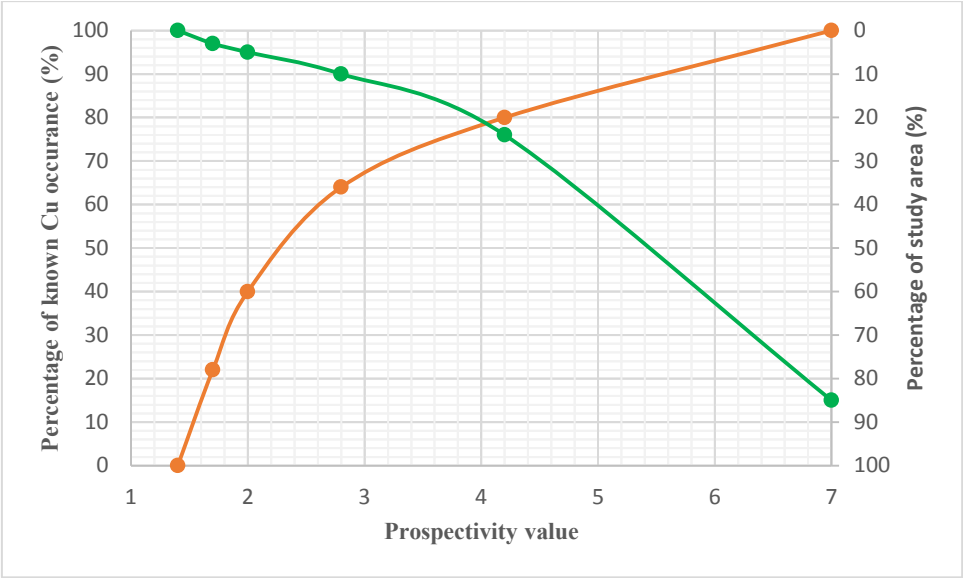

(a)

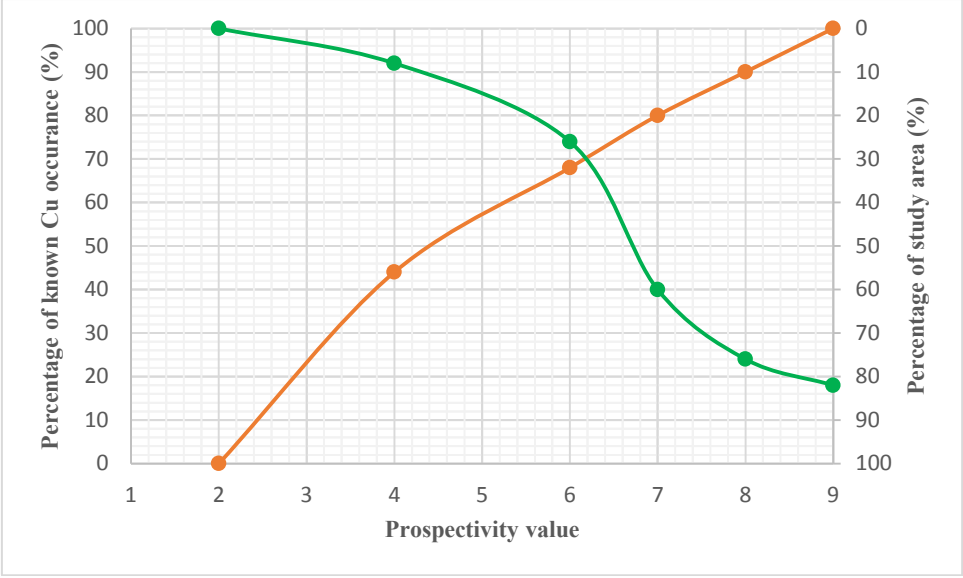

(b)

Figure 12. P-A plot for prospectivity model generated by a) ANN and b) FL integration methods.

Table 4. Extracted parameters from intersection point of P-A plots.

Integration model	Prediction rate (%)	Occupied area (%)
ANN	80	20
FL	70	30

7. Conclusions

Due to the importance of MPM to minimize the cost and time as well as maximizing the benefit of a mineral exploration program and also decreasing the uncertainty caused by the unknown/complex geological variables, a mining engineer and exploration geologist should be able to apply a robust and transparent method to determine the favorable zones of mineralization for further exploration. For this purpose, two techniques of knowledge-driven fuzzy and data-driven ANN were employed for predicting favorable areas associated with the Cu mineralization in the Shahr-e-Babak area, Kerman Province, SE Iran. We used solid lithology, tectonic (faults and dykes), airborne total magnetic intensity, airborne gamma-ray spectrometry data (U, Th, K, and total count), remotely-sensed data (hydrothermal alteration haloes), geochemical data, plus 34 deposits/occurrences representing known Cu mineralizations as the evidential maps. The results obtained indicate that in this particular application, the ANN method produces a plausible mineral prospectivity map from the geological

aspect and superior to the FL map. The ANN method is regarded as the objective because it is data-driven, and it is not necessary to select the weights based on the researcher's knowledge. The fuzzy method, on the other hand, depends on a reliable and correct exploration model. In this work, the ANN data-driven approach due to the capabilities such as classification, pattern matching, optimization, and prediction shows better results than the FL knowledge-driven technique so that the areas with moderate-to-low favorability that are candidates for further exploration are detected very well with this method, while FL failed to identify them.

References

[1]. Zuo, R. and Carranza, E.J.M. (2011). Support vector machine: a tool for mapping mineral prospectivity. Comput Geosci. 37: 1967-1975.

[2]. Shabankareh, M. and Hezarkhani, A. (2017). Application of support vector machines for copper potential mapping in Kerman region, Iran. J Afr Earth Sci. 128: 116-126.

[3]. Pan, G. (1993). Canonical favorability model for data integration and mineral potential mapping. Comput Geosci. 19: 1077-1100.

[4]. Joly, A., Porwal, A. and McCuaig, T.C. (2012). Exploration targeting for orogenic gold deposits in the Granites-Tanami Orogen: mineral system analysis, targeting model and prospectivity analysis. Ore Geol Rev. 48: 349-383.

[5]. Bonham-Carter, G.F. (1994). Geographic Information Systems for Geoscientists: modelling with GIS. Pergamon, Ontario.

[6]. Chen, Y. and Wu, W. (2016). A prospecting cost-benefit strategy for mineral potential mapping based on ROC curve analysis. Ore Geol Rev. 74: 26-38.

[7]. Choi, S., Moon, W.M. and Choi, S.G. (2000). Fuzzy logic fusion of W-Mo exploration data from Seobyeog-ri, Korea. Geosci J. 4: 43-52.

[8]. Abedi, M., Norouzi, G.H. and Bahroudi, A. (2012). Support vector machine for multi-classification of mineral prospectivity areas. Comput Geosci. 46: 272-283.

[9]. Najafi, A., Karimpour, M.H. and Ghaderi, M. (2014). Application of fuzzy AHP method to IOCG prospectivity mapping: A case study in Taherabad prospecting area, eastern Iran. Int J Appl Earth Obs Geoinf. 33: 142-154.

[10]. Yousefi, M. and Carranza, E.J.M. (2015). Geometric average of spatial evidence data layers: a GIS-based multi-criteria decision-making approach to mineral prospectivity mapping. Comput Geosci. 83: 72-79.

[11]. Carranza, E.J.M. (2008). Geochemical anomaly and mineral prospectivity mapping in GIS: Elsevier.

[12]. Bonham-Carter, G.F. (2014). Geographic information systems for geoscientists: modelling with GIS: Elsevier.

[13]. Leite, E.P. and de Souza Filho, C.R. (2009). Artificial neural networks applied to mineral potential mapping for copper-gold mineralizations in the Carajás Mineral Province, Brazil. Geophys Prospec. 57: 1049-1065.

[14]. Luo, X. and Dimitrakopoulos, R. (2003). Data-driven fuzzy analysis in quantitative mineral resource assessment. Comput Geosci. 29: 3-13.

[15]. Nykänen, V., Groves, D., Ojala, V. and Gardoll, S. (2008). Combined conceptual/empirical prospectivity mapping for orogenic gold in the northern Fennoscandian Shield, Finland. Aust J Earth Sci. 55: 39-59.

[16]. Chen, C., Dai, H., Liu, Y. and He, B. (2011). Mineral prospectivity mapping integrating multi-source geology spatial data sets and logistic regression modelling. Spatial Data Mining and Geographical Knowledge Services (ICSDM), 2011 IEEE Int Conf IEEE. pp. 21-47.

[17]. Agterberg, F.P. (1992). Combining indicator patterns in weights of evidence modeling for resource evaluation. Nat Resour Res1. pp. 39-50.

[18]. Raines, G.L. (1999). Evaluation of weights of evidence to predict epithermal-gold deposits in the great basin of the western United States. Nat Resour Res. 8: 257-276.

[19]. Zahiri, H., Palamara, D., Flentje, P., Brassington, G.M. and Baafi, E. (2006). A GIS-based weights-of-evidence model for mapping cliff instabilities associated with mine subsidence. Envi Geol. 51: 377-386.

[20]. Lee, S., Oh, H.J., Heo, C.H. and Park, I. (2014). A case study for the integration of predictive mineral potential maps. Open Geosci. 6: 373-392.

[21]. Porwal, A., Carranza, E. and Hale, M. (2001). Extended weights-of-evidence modelling for predictive mapping of base metal deposit potential in Aravalli province, western India. Explor Min Geol. 10: 273-387.

[22]. Porwal, A., Carranza, E. and Hale, M. (2003). Knowledge-driven and data-driven fuzzy models for predictive mineral potential mapping. Nat Resour Res. 12: 1-25.

[23]. Carranza, E.J.M. (2015). Data-driven evidential belief modeling of mineral potential using few prospects and evidence with missing values. Nat Resour Res. 24: 291-304.

[24]. Liu, Y., Cheng, Q., Xia, Q. and Wang, X. (2015). The use of evidential belief functions for mineral

potential mapping in the Nanling belt, South China. Front Earth Sci. 9: 342-354.

[25]. Porwal, A., Carranza, E.J.M. and Hale, M. (2006). Bayesian network classifiers for mineral potential mapping. Comput Geosci. 32: 1-16.

[26]. Porwal, A., Carranza, E.J.M. and Hale, M. (2006). A hybrid fuzzy weights-of-evidence model for mineral potential mapping. Nat Resour Res. 15: 1-14.

[27]. Brown, W.M., Gedeon, T., Groves, D. and Barnes, R. (2000). Artificial neural networks: a new method for mineral prospectivity mapping. Aust j earth sci. 47: 757-570.

[28]. Skabar, A. (2007). Mineral potential mapping using Bayesian learning for multilayer perceptrons. Math Geol. 39: 439-451.

[29]. Nykänen, V. (2008). Radial basis functional link nets used as a prospectivity mapping tool for orogenic gold deposits within the Central Lapland Greenstone Belt, Northern Fennoscandian Shield. Nat Resour Res. 17: 29-48.

[30]. Singer, D.A. and Kouda, R. (1999). A comparison of the weights-of-evidence method and probabilistic neural networks. Nat Resour Res. 8: 287-298.

[31]. Leite, E.P. and de Souza Filho, C.R. (2009). Probabilistic neural networks applied to mineral potential mapping for platinum group elements in the Serra Leste region, Carajás Mineral Province, Brazil. Comput Geosci. 35: 675-687.

[32]. Chen, Y. (2015). Mineral potential mapping with a restricted Boltzmann machine. Ore Geol Rev. 71: 749-760.

[33]. Beucher, A., Fröjdö, S., Österholm, P., Martinkauppi, A. and Edén, P. (2014). Fuzzy logic for acid sulfate soil mapping: Application to the southern part of the Finnish coastal areas. Geoderma. 226: 21-30.

[34]. Kashani, S.B.M., Abedi, M. and Norouzi, G.H. (2016). Fuzzy logic mineral potential mapping for copper exploration using multi-disciplinary geo-datasets, a case study in seridune deposit, Iran. Earth Sci Inform. 9 (2): 167-181.

[35]. Bonham-Carter, G., Agterberg, F. and Wright, D. (1988). Integration of geological datasets for gold exploration in Nova Scotia. Digit Geolo Geograph Inform Sys. 1: 15-23.

[36]. Carranza, E.J.M. (2010). Improved wildcat modelling of mineral prospectivity. Resour Geol. 60: 129-149.

[37]. Abedi, M., Norouzi, G.H. and Fathianpour, N. (2013). Fuzzy outranking approach: a knowledge-driven method for mineral prospectivity mapping. Int J Appl Earth Obs Geoinf. 21: 556-567.

[38]. Cheng, Q. and Agterberg, F. (1999). Fuzzy weights of evidence method and its application in mineral potential mapping. Nat Resour Res. 8: 27-35.

[39]. Porwal, A., Carranza, E. and Hale, M. (2004). A hybrid neuro-fuzzy model for mineral potential mapping. Math geol. 36: 803-826.

[40]. Yousefi, M. and Carranza, E.J.M. (2015). Fuzzification of continuous-value spatial evidence for mineral prospectivity mapping. Comput Geosci. 74: 97-109.

[41]. Yousefi, M. and Carranza, E.J.M. (2016). Data-driven index overlay and Boolean logic mineral prospectivity modeling in greenfields exploration. Nat Resour Res. 25: 3-18.

[42]. Geological Survey of Iran. (1973). Exploration for ore deposits in Kerman region, Report no. Yu/53.

[43]. Dimitrijevic, M.D. (1973). Geology of the Kerman region, Report no. Yu/52. Geological Survey of Iran.

[44]. Hezarkhani, A. (2008). Hydrothermal evolution of the Miduk porphyry copper system, Kerman, Iran: a fluid inclusion investigation. Int Geol Rev. 50 (7): 665-684.

[45]. Haykin, S. (1994). Neural networks: a comprehensive foundation: Prentice Hall PTR.

[46]. Samanta, B. and Bandopadhyay, S. (2009). Construction of a radial basis function network using an evolutionary algorithm for grade estimation in a placer gold deposit. Comput Geosci. 35: 1592-1602.

[47]. Chang, F.J., Kao, L.S., Kuo, Y.M. and Liu, C.W. (2010). Artificial neural networks for estimating regional arsenic concentrations in a blackfoot disease area in Taiwan. J hydro. 388: 65-76.

[48]. Abedi, M., Norouzi, G.H. and Torabi, S.A. (2013). Clustering of mineral prospectivity area as an unsupervised classification approach to explore copper deposit. Arab J Geosci. 6: 3601-3613.

[49]. Rojas, R. (2013). Neural networks: a systematic introduction: Springer Science & Business Media.

[50]. Szymczyk, P. and Szymczyk, M. (2015). Classification of geological structure using ground penetrating radar and Laplace transform artificial neural networks. Neurocomputing. 148: 354-362.

[51]. Kasabov, N. (1996). Foundations of neural networks, fuzzy logic and knowledge engineering. MIT Press, Cambridge.

[52]. Zadeh, L.A. (1965). Fuzzy sets. Inform cont. 8: 338-353.

[53]. Kandel, A. (1986). Fuzzy mathematical techniques with applications.

[54]. An, P. (1991). Application of fuzzy set theory to integrated mineral exploration. Can J Explor Geophys. 27: 1-11.

[55]. Rahman, S.M. and Ratrout, N.T. (2009). Review of the fuzzy logic based approach in traffic signal control: prospects in Saudi Arabia. J trans Sys eng inform Techn. 9: 58-70.

[56]. Akumu, C., Johnson, J., Etheridge, D., Uhlig, P., Woods, M. and Pitt, D. (2015). GIS-fuzzy logic based approach in modeling soil texture: using parts of the Clay Belt and Hornepayne region in Ontario Canada as a case study. Geoderma. 239: 13-24.

[57]. Zhang, N., Zhou, K. and Du, X. (2017). Application of fuzzy logic and fuzzy AHP to mineral prospectivity mapping of porphyry and hydrothermal vein copper deposits in the Dananhu-Tousuquan island arc, Xinjiang, NW China. J Afr Earth Sci. 128: 84-96.

[58]. Ganiyu, S., Badmus, B., Awoyemi, M., Akinyemi, O. and Olurin, O.T. (2012). Upward continuation and reduction to pole process on aeromagnetic data of Ibadan Area, South-Western Nigeria. Earth Sci Res. 2: 66.

[59]. Tangestani, M. and Moore, F. (2003). Mapping porphyry copper potential with a fuzzy model, northern Shahr-e-Babak, Iran. Aust J Earth Sci. 50: 311-317.

[60]. Briggs, I.C. (1974). Machine contouring using minimum curvature. Geophysics. 39: 39-48.

[61]. Aitchison, J. (1986). The statistical analysis of compositional data.

[62]. Mahmoudabadi, H., Izadi, M. and Menhaj, M.B. (2009). A hybrid method for grade estimation using genetic algorithm and neural networks. Comput Geosci. 13: 91-101.

[63]. Li, X.L., Li, L.H., Zhang, B.L. and Guo, Q.J. (2013). Hybrid self-adaptive learning based particle swarm optimization and support vector regression model for grade estimation. Neurocomputing. 118: 179-190.

[64]. Chaturvedi, D., Satsangi, P. and Kalra, P. (1996). Effect of different mappings and normalization of neural network models. Proceedings of the National Power Systems Conference: Indian Institute of Technology. pp. 377-386.

[65]. Sola, J. and Sevilla, J. (1997). Importance of input data normalization for the application of neural networks to complex industrial problems. IEEE Trans Nucl Sci. 44: 1464-1468.

[66]. Demuth, H.B., Beale, M.H., De Jess, O. and Hagan, M.T. (2014). Neural network design: Martin Hagan.

[67]. Sreekanth, P., Geethanjali, N., Sreedevi, P., Ahmed, S., Kumar, N.R. and Jayanthi, P.K. (2009). Forecasting groundwater level using artificial neural networks. Curr sci. 933-939.

[68]. De Smith, M.J., Goodchild, M.F. and Longley, P.A. (2007). Geospatial analysis- a comprehensive guide to principles, techniques and software tools, 3rd edition.

[69]. Porwal, A., Carranza, E.J.M. and Hale, M. (2003). Artificial neural networks for mineral potential mapping; a case study from Aravalli Province, Western India. Natural Resources Research. 12 (3): 155-171.

[70]. Chang, F.J., Kao, L.S., Kuo, Y.M. and Liu, C.W. (2010). Artificial neural networks for estimating regional arsenic concentrations in a blackfoot disease area in Taiwan. Journal of hydrology. 388 (1-2): 65-76.

[71]. Kasabovn. K. (1996). Foundations of Neural Networks, Fuzzy Logic and Knowledge Engineering. MIT Press, Cambridge.

[72]. Bonham-Carter, G.F. (1994). Geographic Information Systems for Geoscientists: Modelling with GIS. Computer Methods in the Geosciences 13. Pergamon Press, New York.

[73]. Pazand, K., Hezarkhani, A. and Ghanbari, Y. (2014). Fuzzy analytical hierarchy process and GIS for predictive Cuporphyry potential mapping: a case study in AharArasbaranZone (NW, Iran). Arab. J. Geosci. 7: 241-251.

[74]. Cheng, Q., Chen, Z. and Khaled, A. (2007). Application of fuzzy weights of evidence methodin mineral resource assessment for gold in Zhenyuan District, Yunnan Province,China. Earth Sci. J. China Univ. Geosci. 32 (2): 175-184.

[75]. Takagi, T. and Sugeno, M. (1985). Fuzzy identification of systems and its applications to modeling and control. IEEE Transactions on Systems, Man, and Cybernetics. 15 (1): 116-132.

[76]. Parsa, M., Maghsoudi, A., Yousefi, M. and Sadeghi, M. (2016). Prospectivity modeling of porphyry-Cu deposits by identification and integration of efficient mono-elemental geochemical signatures. J Afr Earth Sci. 114: 228-241.

[77]. Yousefi, M. and Carranza, E.J.M. (2015). Prediction-area (P-A) plot and C-A fractal analysis to classify and evaluate evidential maps for mineral prospectivity modeling. Comput Geosci. 79: 69-81.

مقایسه بین روش‌های دانش‌محور فازی و داده محور شبکه عصبی مصنوعی برای پی‌جویی کانی‌زایی مس؛ مطالعه موردی: ناحیه شهر بابک، استان کرمان، جنوب شرق ایران

بشیر شکوه سلجوقی، اردشیر هزارخانی* و احسان فرح‌بخش

دانشکده مهندسی معدن و متالورژی، دانشگاه صنعتی امیرکبیر، ایران

ارسال ۲۰۱۸/۲/۵، پذیرش ۲۰۱۸/۶/۱۹

* نویسنده مسئول مکاتبات: ardehez@aut.ac.ir

چکیده:

ناحیه مطالعاتی واقع شده در بخش جنوبی کمپلکس رسوبی- آتش‌فشانی ایران مرکزی، حاوی تعداد زیادی نهشته‌ها و رخدادهای معدنی است که در حال حاضر با کمبود منابع مواجهه است؛ بنابراین، پی‌جویی نواحی بالقوه در فضاهای عمیق‌تر و پیرامونی اولویت اصلی در این ناحیه است. روش‌های مستقیم و غیرمستقیم مختلف سعی در پیش‌بینی نواحی امیدبخش برای اکتشافات آتی دارند که اغلب آن‌ها زمان‌بر و پرهزینه هستند. هدف اصلی پی‌جویی مواد معدنی به کار بردن روشی شفاف و معتبر برای شناسایی نواحی بالقوه برای اکتشاف در آینده است. این پژوهش فرآیند به کار رفته برای ایجاد دو نقشه مطلوبیت کانی‌سازی مس را نشان می‌دهد. نخستین نقشه با استفاده از روش فازی دانش‌محور و دومین نقشه توسط روش شبکه عصبی داده محور ترسیم شد. در این پژوهش، هدف بررسی نتایج به کار بردن شبکه عصبی و مقایسه آن با خروجی‌های روش منطق فازی است. پایگاه داده علوم زمین به کار برده شده برای ایجاد نقشه‌های نشانگر کانی‌سازی مس پورفیری شامل نقشه‌های زمین‌شناسی، دگرسانی، گسل‌ها، دایک‌ها، شدت مغناطیس هوابرد، داده‌های طیف‌سنجی اشعه گاما هوابرد (اورانیوم، توریم، پتاسیم و شمارش کل) و رخدادهای شناخته شده مس می‌باشند. بر اساس این پژوهش، روش شبکه عصبی تخمین‌گر بهتری برای کانی‌سازی مس نسبت به روش منطق فازی است. روش شبکه عصبی مصنوعی با توجه به داشتن قابلیت‌هایی مانند طبقه‌بندی، تطبیق الگو، بهینه‌سازی و پیش‌بینی در شناسایی آنومالی‌های مرتبط با کانی‌سازی مس سودمند است.

کلمات کلیدی: تهیه نقشه پتانسیل معدنی، شبکه عصبی مصنوعی، منطق فازی، کانی‌زایی مس، شهر بابک.